Turk J Phys
30 (2006) , 221 – 229.

Computational Studies on Mechanical Properties of Carbon Nanotori

Tahir ÇAĞIN[1], Guanghua GAO[2], William A. GODDARD, III[2]
[1] *Texas A&M University, Artie McFerrin Department of Chemical Engineering, 519 Jack E. Brown Engineering Building, 3122 TAMU, College Station, TX 77843-3122, USA*
[2] *Materials and Process Simulation Center, California Institute of Technology, Pasadena, CA 91125, USA*

Received 18.07.2006

Abstract

Carbon has diverse structures, especially (0-dimensional) fullerenes, (1-dimensional) tubes have generated great interest among scientists and technologists. Studies of the structures and properties of these low dimensional carbon molecules show tremendous potential for use in nanoscale device applications. Motivated by these exciting possibilities in finding new forms of carbon materials and their potential applications, we have designed hypothetical single wall carbon nano-toroids. Carbon toroids are also ideal in studying the elastic and plastic deformation behavior of nanotubes under bending loads. We can accurately correlate the behavior of the tubes to its uniform curvature. In this particular work we focused on the rings of (10,10) tubes and studied their energetics, structure and mechanical properties as a function of their toroidal radius. Especially important, we have observed specific strain release paths for the toroids, i.e. the toroids going through plastic deformations and nucleating a number of kinks. We have studied phase stability diagram of toroids with kinks as a function of ring radius.

1. Introduction

Carbon has diverse forms of structure [1, 2] both in nature and by lab synthesize. Three dimensional diamond and two dimensional graphite sheet are the two well-known forms. In the past decade, the discoveries of zero dimensional bucky balls [3–7] and one dimensional bucky tubes [8, 9] have generated great interests among researchers. Studies of the structures and properties of low-dimensional carbon molecules, theoretical [10–13] and experimental [14–18] showed tremendous potential use of nano scale carbon material as components of electro-magnetic devices, or high yielding materials. Among them, experiments done by Dai [19] and Wang [20] illustrated the potential use of carbon nano tube as scanning microscopic probe. Motivated by these exciting development in finding new forms of carbon materials and studies of their properties, among others [21, 22] we proposed and designed a hypothetical carbon molecules, single walled carbon nano toroids [23]. Carbon toroids system is an ideal model for studying the behavior of single walled nano tubes under bending. We can accurately correlate the behavior of the tubes to its uniform curvature. Since then various groups has observed circular ropes of single wall carbon nanotubes [24, 25]. From technological applications point of view, pure, or doped (inside the tube by other elements) forms of carbon toroids could be synthesized and find its use as components of electro-magnetic devices or micro machines, e.g., as nano conducting rings. They are expected to have interesting diamagnetic properties as well [26].

The carbon toroid can be characterized by three integers (n, m, l), where (n, m) defines the single-walled nano tube that is used to construct the toroid, while l is the number of the smallest repeating units along tube axis. We investigated the mechanical property of carbon toroids to investigate the bending of (10, 10) single-walled carbon nano tube.

Figure 1. Starting structure of two toroids with different radii, the smallest stable toroid and the largest toroid used in our calculation.

2. Methods and Results

2.1. Force Field Parameters Used for Carbon Nano Toroids

We generated toroids with radius from 19.43 Å that is (10, 10, 100) with 2,000 atoms, to 388.69 Å, (10, 10, 2000) with 40,000 atoms. Based on the molecular simulation force field (MSFF) [27], their structures are optimized by using molecular mechanics and molecular dynamics. Developed for graphite and fullerenes, MSFF was proved to be very accurate in calculating vibration frequencies and predicting experimental structures. The parameters are listed in Table and Figure 1 show the initial structures of two toroids, R=38.87 Å of (10, 10, 200), and R=388.7 Å of (10, 10, 2000).

The Van der Waals energy is given through Lennard-Jones form

$$E_{vdw} = D_o(\frac{1}{\rho^{12}} - \frac{2}{\rho^6}),$$

where $\rho = \frac{r}{r_v}$ and r_v is the separation at minimum energy, and r is the distance between two atoms. The bond stretch energy defined via shifted Morse potential:

$$E_{bond} = D_b(\chi - 1)^2,$$

with $\chi = e^{-(r-r_b)}$, r_b is the equilibrium bond length and r is the current bond length. Angle bending energy is the sum of harmonic bending and stretch-bend coupling:

$$\begin{aligned} E_{angle} &= \frac{1}{2}k_\theta(cos\theta - cos\theta_a)^2 + k_{1\theta}(r_1 - r_{1\theta})(cos\theta - cos\theta_a) && (1) \\ &\quad +k_{2\theta}(r_2 - r_{2\theta})(cos\theta - cos\theta_a) + k_{12}(r_1 - r_{1\theta})(r_2 - r_{2\theta}), && (2) \end{aligned}$$

Table. Force Field Parameters for the carbon nanotube.

Van der Waals	R_v	D_v	Bond	r_e	k_e	E_b
C	3.8050	0.06920	C-C	1.4114	720.0	133.0
Angle	θ_a	k_θ	$k_{1\theta}$	$k_{2\theta}$	k_{12}	
C-C	120.0	196.13	-72.410	-72.410	68.0	
Torsional	V_o	V_1	V_2			
C-C-C-C	10.64	0.0	-10.64			

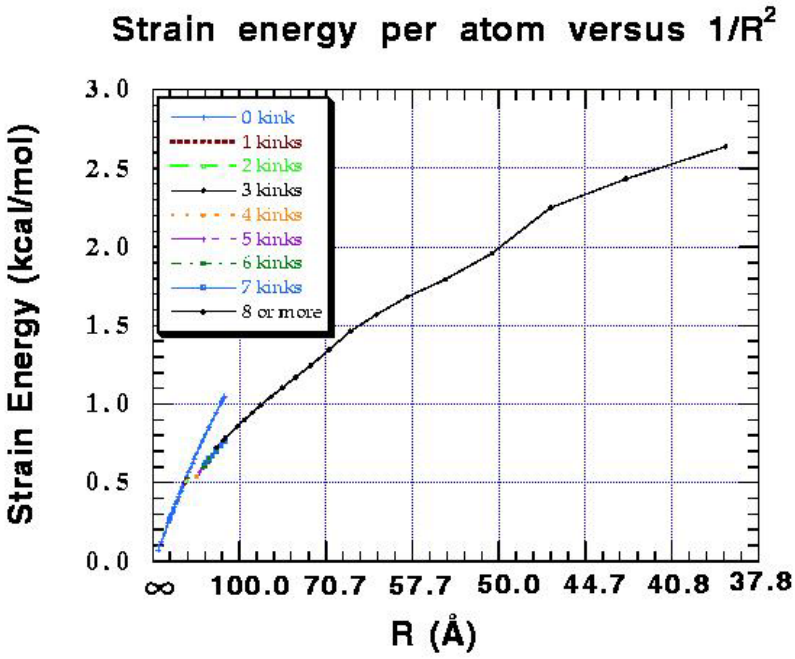

Figure 2. Strain energy per atom versus curvature

where $k_\theta, k_{1\theta}, k_{2\theta}$, and k_{12} are the bond stretch and stretch-bend force constants defined for the angle θ with equilibrium value θ_a and $r_{1\theta}, r_{2\theta}$ are the equilibrium bond lengths for the first and second bonds forming the angle θ. Finally, the dihedral angle energy between four bonded atoms is given by

$$E_{dihedral} = V_o + V_1 cos\phi + V_2 cos(2\phi)\,,$$

as the truncated Fourier expansion up to second order, V_o, V_1 and V_2 are the expansion coefficients.

2.2. Structures of Toroids

Toroids with small radius are highly strained. To stabilize the structure, harmonic bond interactions are used at the early stage of the minimization. The more accurate Morse potential that allows bond breaking are then used at the latter stage of minimization. By doing so, we can avoid the bias built in when the starting structure was created. This is important for tracking down the transition radius that separates stable toroids (though highly strained) from the unstable toroids (under Morse bond interaction, the structure flies apart). Figure 2. is the strain energy per atom (relative to infinite long straight (10, 10) tube) versus $\frac{1}{R^2}$. For toroids with different radius, different final structures resulted. In the plot, we can identify three transition radii, associated with four structural regions.

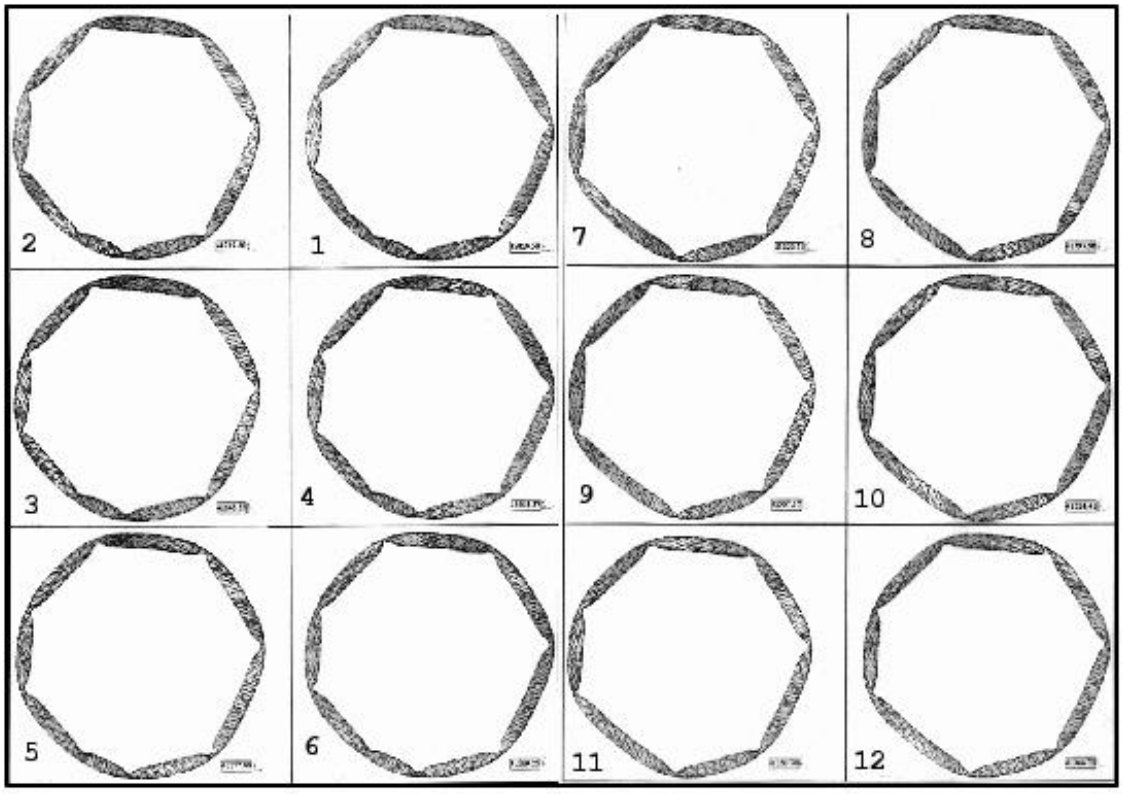

Figure 3. Snapshots of structural minimization; numbered according to the minimization stages to illustrate nucleation of small buckles into large buckle

For toroids with radii larger than $R_s = 183.3$ Å (corresponds to (10, 10, 943) toroid with 18,860 atoms), after molecular dynamics simulation and energy minimization, smooth toriod is the only stable structure. This corresponds to the elastic bending of isolated (10, 10) tube.

For toroids with radii smaller than $R_s = 183.3$ Å and larger than 109.6 Å ((10, 10, 564) with 11280 atoms), the optimum structures obtained through minimization are smooth toroids without buckles. However, after 20 ps of molecular dynamics equilibration at 300 K, numerous small dents appeared along the inner wall. Take a snapshot of dynamics trajectory as the starting point of structural minimization, we found an interesting phenomena. During the minimization, small dents diffused along the inner tube and nucleated into larger dents when they meet. This nucleation of deformations continues, until the optimum structure resulted. The optimum structures usually have a number of buckles almost uniformly spaced along the tube.

In Figure 3 displayed are the snapshots at the late stage of minimization for (10, 10, 564) (toroid with radius of 109.6 Å and 11280 atoms). Looking at the lower left quarter of each ring, we can clearly identify the diffusion of small dents. These small dents eventually moved toward the larger dent as the minimization progresses, and combined with the large dent. The snapshots are numbered according to the minimization sequence. Snapshot with smaller numbering represents structure at earlier stage of minimization. Comparing to the smooth toroids, these structures have lower strain energy per atom. This is due to the stretching of the outer surface and compression of the inner surface. Knee like buckle relaxes compression over large region at the expense of increased local strain.

Figure 4 represents a close look at a buckle, which is cut out from a optimized toroid with one buckle. At the center of the buckle, tube wall collapsed completely. The closest distance between atoms in opposite tube walls is 3.3 Å, comparable to the distance between adjacent layers of graphite. A short distance away

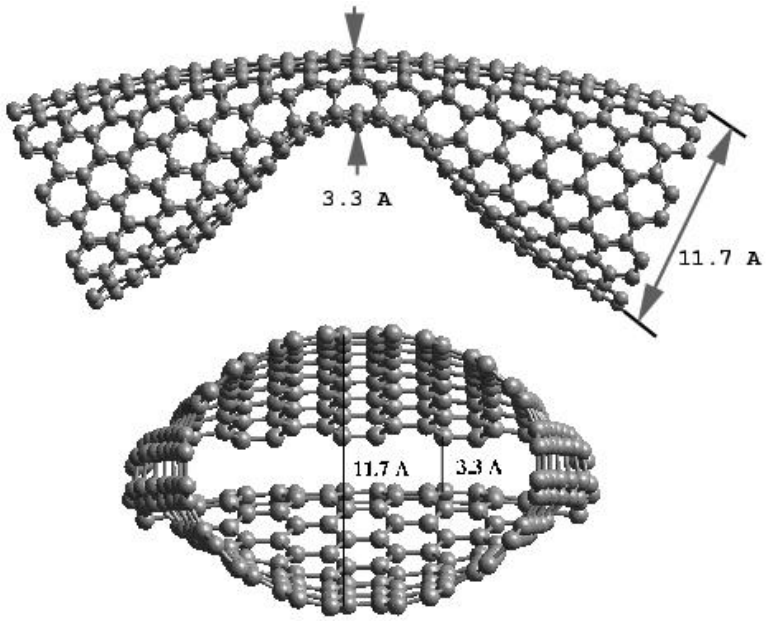

Figure 4. Close look at a buckle

from the collapsed point, the tube stays almost circular. Rooms created for the inner wall at the buckles relax the stretch and compression along the rest of the toroid.

There is a strong correlation between the number of buckles and the curvature of the toroids. The higher the strain (curvature) is, the more buckles appeared in the final structure of minimization. However, for each toroid within this region, there are many stable final structures with different number of buckles, each resulted from different starting structure. This suggests that there exist many meta stable structures for toroids in this region. The fact that the curves towards small radius in Figure 2 are not smooth suggests that we are not connecting the points with optimum number of buckles. Generally, if we increase the radius (thus reduce strain) we get structures with smaller number of buckles and when we approach the smooth region, we should get only structures with single buckle.

In order to track down the transition point, we created structures with different number of buckles as starting point of minimization. The buckles are uniformly distributed along the circumferences. To create a buckle, we added artificial harmonic constraint on two atoms in the opposite wall of the tube to pull together the inner wall and the outer wall. After the structures are minimized to lower RMS force, where the structures are stable under Morse bond interaction, we remove the constraints and switch harmonic bond potential back to Morse potential to further optimize the structures. We could just heat up the initial structures by using molecular dynamics and then anneal them down to zero temperature. However, given the size of the toroids in the transition, the long time that takes to anneal each structure, and the fact that there could be several stable structures associated with different number of buckles, it is impractical to do so.

Figure 5 shows the transition region where smooth toroids and toroids with different number of buckles co-exist. Points with same number of buckles are connected into lines. It clearly shows the overlap and shifts of lines with different number of buckles. Towards the transition point beyond which smooth toroids resulted, we are able to create stable structures with four buckles, three buckles, two buckles and one buckle. At region close to the transition radius R_s, only the one buckle toroids have the smallest strain energy per atom. Figure 6 shows the buckled structures in this region.

If we further increase the curvature (decrease radius), at R_k=109.6 Å, (corresponds to (10, 10, 564)

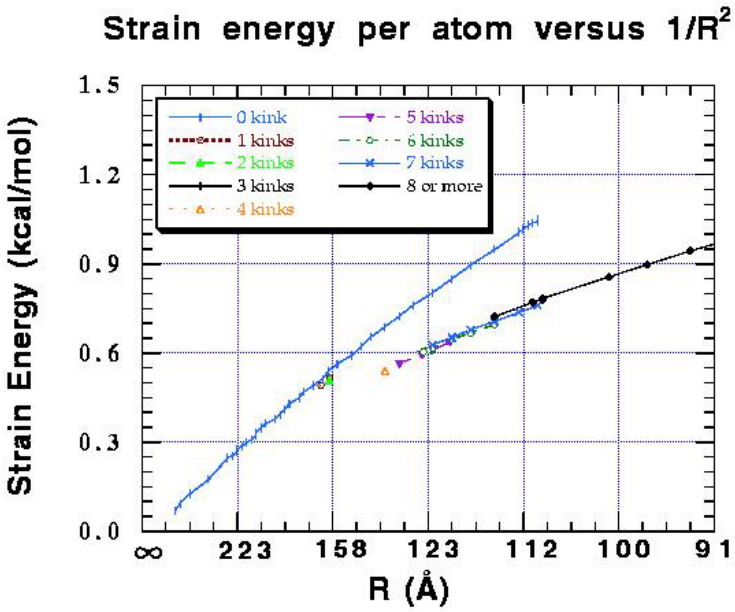

Figure 5. Strain energy per atom versus $\frac{1}{R^2}$ at the transition region where smooth toroids and toroids with different number of buckles co-exist

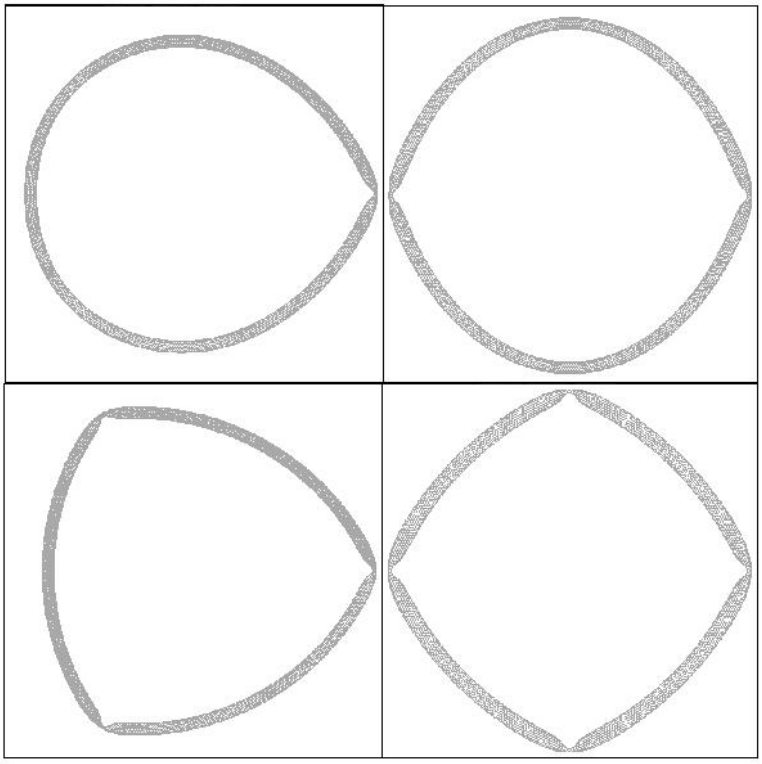

Figure 6. Optimized carbon toroids with 1, 2, 3, and 4 buckles. The single buckle toroid has 16,800 carbon atoms. Denoted as (10,10,840), the radius of its circular form is 163.3 Å. The double-buckle toroid has 16,400 carbon atoms, (10,10,820), its radius of circular form is 159.4 Å. The triple-buckle toroid has 18,000 atoms, (10,10,900), radius of its circular form is 174.9 Å. The toroid with four buckles has 14,400 atoms, (10,10,720), radius of its circular form is 139.9 Å.

toroid with 11,280 atoms), only toroids with various number of buckles exist. At even higher curvature, the toroids are flatterned. In this region, there are no smooth toroids, due to the high strain built in the compression of inner wall and tension of the outer wall. Further decrease the radius down to the point of R_b=38.9 Å (corresponds to (10, 10, 200) toroid with 4,000 atoms), the structure breaks and atoms fly apart in the course of minimization. Figure 7 shows toroids with more than eight buckles to the smallest toroid that can stand the built in strain.

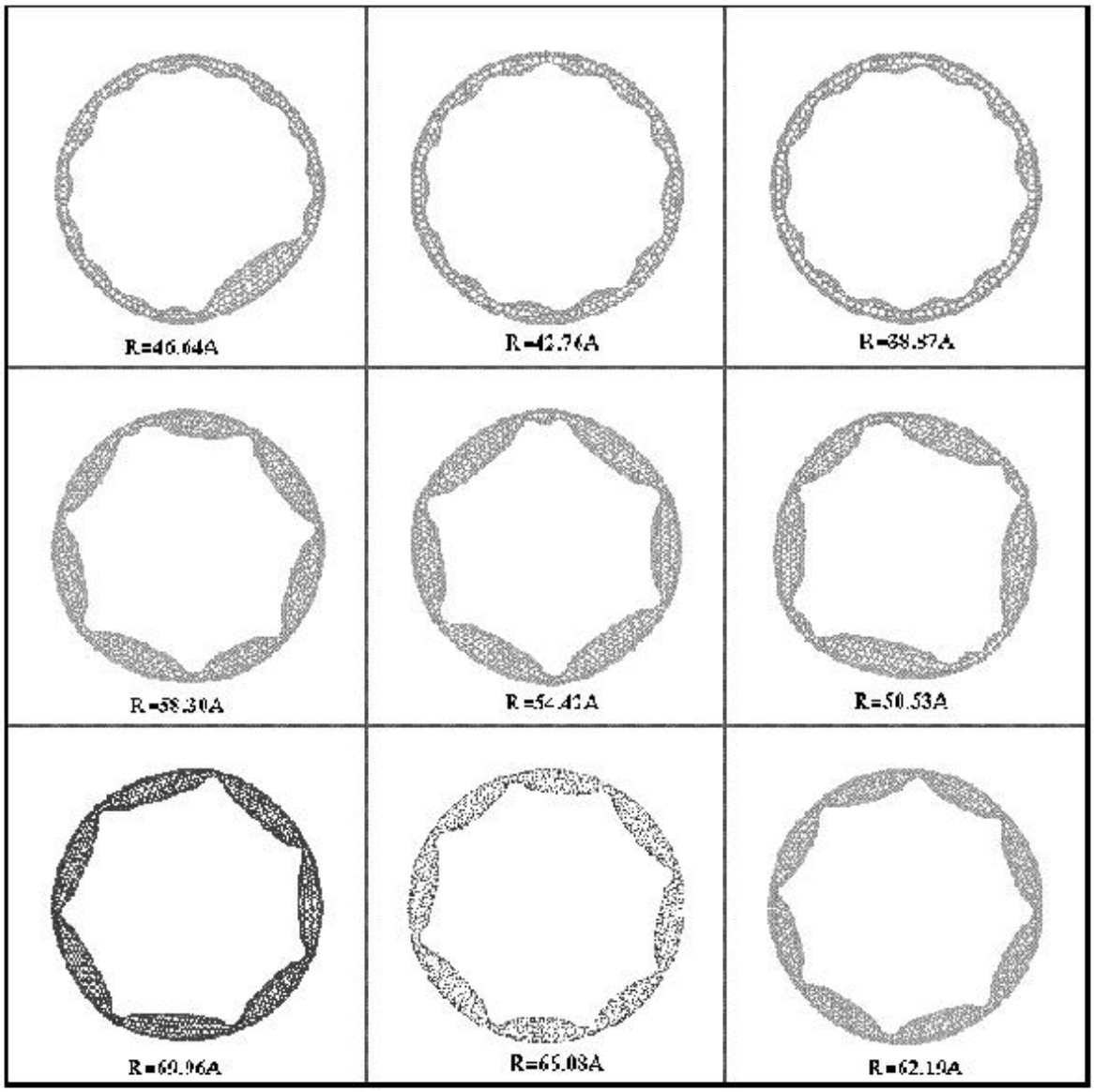

Figure 7. A Collection of buckled toroids

2.3. Mechanical Properties

Consider the (10, 10) tube as thin elastic rods, then the toroids are rings of thin rods. Assuming κ as the Young's modulus of the (10,10) tube, I as the moment of inertia about the axis parallel to tube cross section, the strain energy of the rings are given by

$$E_{strain} = \frac{1}{2}\kappa I \int (\frac{1}{R} - \frac{1}{R_o})^2 dl\,,$$

where

$$I_y = \int x^2 df = \frac{1}{2}\int r^2 df = \frac{\pi}{4}(r_{out}^4 - r_{in}^4)\,.$$

Taking r_{out} = 16.70 Å, the inter-tube distance of (10, 10) SWNT crystals, r_{in} = 10.5 Å, which assumes 13.6 as the radius of (10, 10) tube, we get Young's modulus of the 913 GPa for toroids of large radius.

3. Concluding Remarks

We have investigated energetics and structures of (10, 10, n) toroids, three transition radii are found that define the regions with different stable structures. Below R_b=38.9 Å, there is no stable (10,10,l) single wall nano rings, between R_b=38.9 Å and R_k=109.6 Å only the toroids with buckles are stable. With R_s=183.3 Å, between R_k and R_s both circular and kinked structures are stable. In this region the kinked ones are energetically more favorable. Above R_s, the circular structures are energetically favorable, but structures with kinks are also possible. The optimum number of buckles for each structure evolves through the propagation of buckles and their coalescence to new ones on the inner portion of the tori. Based on classical elastic theory analysis, we calculated the modulus of different regions. The calculated Young's modulus along the tube axis of (10,10) tube is found to be 913 GPa from these calculations.

References

[1] D. R. Huffman, *Physics Today*, **44**, (1991), 22.

[2] G. G. Tibbetts, *J. Cryst. Growth,* **66**, (1984), 632.

[3] H. W. Kroto, J. R. Heath, S. C. O'Brien, R. F. Curl, R. E. Smalley, *Nature*, **318**, (1985), 162.

[4] W. Kratschmer, L. D. Lamb, K. Fostiropoulos, and D. R. Huffman, *Nature*, **347**, (1990), 354.

[5] D. S. Bethune, G. Meijer, W. C. Tang, H. J. Rosen, *Chem. Phys. Lett.*, **174**, (1990), 219.

[6] W. Kratschmer, K. Fostiropoulos, and D. R. Huffman, *Chem. Phys. Lett.*, **170**, (1990), 167

[7] R. Taylor, J. P. Hare, A. K. Abdul-Sade, and H. W. Kroto, *J. Chem. Soc. Chem. Comm.*, **20**, (1990), 1423.

[8] S. Iijima, *Nature*, **354**, (1991), 56.

[9] D. S. Bethune, C. H. Kiang, M. S. Devries, G. Gorman, R. Savoy, J. Vazquez, R. Beyers, *Nature*, **363**, (1993), 605.

[10] M. S. Dresselhaus, G. Dresselhaus, and R. Saito, *Carbon*, **33**, (1995), 883.

[11] R. A. Jishi, D. Inomata, K. Nakao, M. S. Dresselhaus, and G. Dresselhaus, *J. Phys. Soc. Japan*, **63**, (1994), 2252.

[12] L. X. Benedict, V. H. Crespi, S. G. Louie, and M. L. Cohen, *Phys. Rev. B,* **52**, (1995), 14935.

[13] D. H. Robertson, D. W. Brenner, and J. W. Mintmire, *Phys. Rev. B*, **45**, (1992), 12592.

[14] J. C. Hulteen, H. X. Chen, C. K. Chambliss, and C. R. Martin, *Nano-Structured Materials*, **9**, (1997), 133.

[15] R. S. Ruoff, J. Tersoff, D. C. Lorents, S. Subramoney, and B. Chan, *Nature*, **364**, (1993), 514.

[16] A. Thess, R. Lee, P. Nikolaev, H. Dai, P. Petit, J. Robert, C. Xu, Y. H. Lee, S. G. Kim, A. G. Rinzler, D. T. Colbert, G. E. Scuseria, D. Tomanek, J. E. Fischer, R. E. Smalley, *Science*, **273**, (1996), 483.

[17] M. Bockrath, D. H. Cobden, P. L. McEuen, N. G. Chopra, A. Zettl, A. Thess, and R. E. Smalley, *Science*, **274**, (1997), 1922.

[18] J. M. Cowley, P. Nikolaev, A. Thess, and R. E. Smalley, *Chem. Phys. Lett.*, **265**, (1997), 379.

[19] H. Dai, E. W. Wong, and C. M. Lieber, *Science*, **272**, (1996), 523.

[20] E. W. Wong, P. E. Sheehan, and C. M. Lieber, *Science*, **277**, (1997), 1971.

[21] B. I. Dunlap, *Phys. Rev. B*, **46**, (1992), 1933.

[22] S. Itoh, S. Ihara, and J. I. Kitami, *Phys. Rev. B*, **47**, (1993), 1703

[23] G. H. Gao, T. Cagin, W. A. Goddard, III, *Foresight Conference*, 1999.

[24] S. Liu, et al. *Nature*, **385**, (1997), 780.

[25] M. Sano, A. Kamino, J. Okamura, and S. Shinkai, *Science*, **293**, (2000), 1299.

[26] E. C. Kirby, M. Luo, D. Yan, H. Ying, and W. Li, *Phys. Rev. B*, **51**, (1995), 13833.

[27] Y. J. Guo, N. Karasawa, and W. A. Goddard III, *Nature*, 351, (1991), 464.